Unclassified

SECURITY CLASSIFICATION OF THIS PAGE *(When Data Entered)*

REPORT DOCUMENTATION PAGE

READ INSTRUCTIONS BEFORE COMPLETING FORM

1. REPORT NUMBER: Special Report 84-23	2. GOVT ACCESSION NO.
3. RECIPIENT'S CATALOG NUMBER	
4. TITLE *(and Subtitle)*: BUCKLING ANALYSIS OF CRACKED, FLOATING ICE SHEETS	5. TYPE OF REPORT & PERIOD COVERED
6. PERFORMING ORG. REPORT NUMBER	
7. AUTHOR(s): M.D. Adley and D.S. Sodhi	8. CONTRACT OR GRANT NUMBER(s)
9. PERFORMING ORGANIZATION NAME AND ADDRESS: U.S. Army Cold Regions Research and Engineering Laboratory, Hanover, New Hampshire 03755	10. PROGRAM ELEMENT, PROJECT, TASK AREA & WORK UNIT NUMBERS: CWIS 31723
11. CONTROLLING OFFICE NAME AND ADDRESS: Office of the Chief of Engineers, Washington, DC 20314	12. REPORT DATE: August 1984
	13. NUMBER OF PAGES: 33
14. MONITORING AGENCY NAME & ADDRESS *(if different from Controlling Office)*	15. SECURITY CLASS. *(of this report)*: Unclassified
	15a. DECLASSIFICATION/DOWNGRADING SCHEDULE

16. DISTRIBUTION STATEMENT *(of this Report)*

Approved for public release; distribution unlimited.

17. DISTRIBUTION STATEMENT *(of the abstract entered in Block 20, if different from Report)*

18. SUPPLEMENTARY NOTES

19. KEY WORDS *(Continue on reverse side if necessary and identify by block number)*

Buckling
Finite element analysis
Ice
Ice sheets

20. ABSTRACT *(Continue on reverse side if necessary and identify by block number)*

A buckling analysis of cracked, floating ice sheets is presented; both symmetrical and unsymmetrical shapes were investigated. The finite element method was used for the in-plane analysis as well as the out-of-plane analysis. The results of the analyses of symmetrically shaped ice sheets are compared to those of previous analyses where a radial stress field was assumed for the in-plane stresses, and there is good agreement between them. The results of theoretical analyses are compared to experimental data obtained in small-scale laboratory experiments.

DD FORM 1 JAN 73 1473 EDITION OF 1 NOV 65 IS OBSOLETE

Unclassified

SECURITY CLASSIFICATION OF THIS PAGE *(When Data Entered)*

PREFACE

This report was prepared by Mark D. Adley, Civil Engineer, and Dr. Devinder S. Sodhi, Research Hydraulic Engineer, both of the Ice Engineering Research Branch, Experimental Engineering Division, U.S. Army Cold Regions Research and Engineering Laboratory.

Funding for this research was provided by Corps of Engineers Civil Works Information Project, CWIS 31723, Model Studies and Ice Effects on Structures. Dr. T.M. Wang of the University of New Hampshire and F. Donald Haynes of CRREL technically reviewed the manuscript of this report.

The contents of this report are not to be used for advertising or promotional purposes. Citation of brand names does not constitute an official endorsement or approval of the use of such commercial products.

Special Report 84-23

August 1984

Buckling analysis of cracked, floating ice sheets

M.D. Adley and D.S. Sodhi

Prepared for
OFFICE OF THE CHIEF OF ENGINEERS

For conversion of SI metric units to U.S./British customary units of measurement consult ASTM Standard E380, Metric Practice Guide, *published by the American Society for Testing and Materials, 1916 Race St., Philadelphia, Pa. 19103.*

CONTENTS

ILLUSTRATIONS

TABLES

BUCKLING ANALYSIS OF CRACKED, FLOATING ICE SHEETS

M.D. Adley and D.S. Sodhi

INTRODUCTION

Background

The design load for offshore structures in northern waters is often the horizontal thrust exerted by a floating ice sheet. The maximum ice force that may be developed is determined by either the environmental driving forces or the force required for the ice sheet to fail. The smaller of these two forces will govern. Since it is very difficult to accurately estimate the magnitude of environmental driving forces such as winds, currents and thermal strains, and since these forces may generally be greater than the failure load of the ice sheet, the force required for the ice sheet to fail is used as an upper limit of the ice forces.

The failure load of the ice sheet is a function of many variables: the strength of the ice sheet, the thickness of the ice sheet, and the type of structure-ice interaction are some of the important factors. These factors will determine the failure mode of the ice sheet. The three most common modes of failure for the ice sheet are bending, crushing and buckling. The bending mode of failure is generally induced by a fixed, rigid structure with sloping sides. The crushing and buckling modes of failure are generally induced by a fixed, rigid, vertical structure, although crushing may also be caused by a fixed, flexible, vertical structure. The buckling mode of failure is most likely to occur when the aspect ratio (structure width/ice thickness) is large, such as when a thin ice sheet impinges on a wide, vertical structure. Conversely the crushing mode of failure is likely to occur when the aspect ratio is small.

When a floating ice sheet is loaded with an in-plane load, cracks may develop from the point of loading and radiate outwards through the ice sheet. As a result of those cracks the domain and the boundary conditions for the differential equation governing the buckling problem are altered. Figure 1

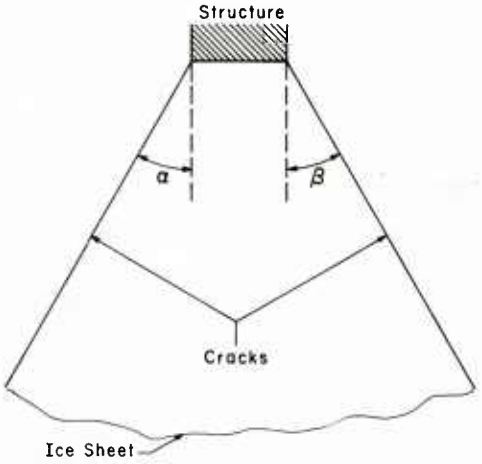

a. Symmetrical configuration of cracks ($\alpha=\beta$).

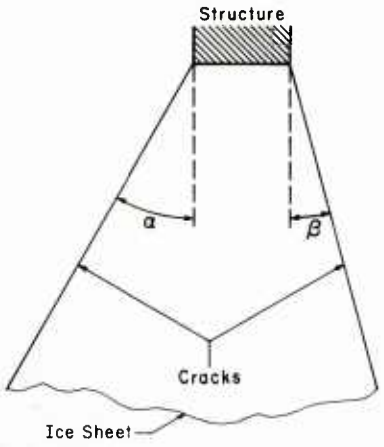

b. Unsymmetrical configuration of cracks ($\alpha\neq\beta$).

Figure 1. Plan view of a floating, cracked ice sheet and a structure as they push each other to produce buckling of an ice sheet.

shows the plan view of a floating ice sheet that is pushed against a structure, resulting in cracks at angles α and β from the edge of a structure. The orientation of cracks will be divided into two groups, those that are symmetrical about the line of loading and those that are not symmetrical about the line of loading. Figures 1a and b, respectively, show examples of a symmetrical and an unsymmetrical configuration of cracks relative to the structure.

After the vertical cracks appear, the largest force the ice sheet can exert on the structure is the failure load of the ice sheet still in contact with the structure. If the aspect ratio is large enough to cause buckling, the largest force the ice sheet can exert on the structure is the buckling load of the cracked, floating ice sheets. The purpose of this study is to determine the buckling load of cracked, floating ice sheets as opposed to crushing failure of ice sheets. The results of theoretical analyses are compared to those determined experimentally. The effect of the ice sheet geometry on the buckling load is determined both theoretically and experimentally. This will be useful in determining the buckling load when a cracked ice sheet interacts with a wide structure.

The theoretical part of the analysis consists of modeling the floating ice sheet as a thin, homogeneous, isotropic, semi-infinite plate resting on an elastic foundation. The force exerted by the elastic foundation is as-

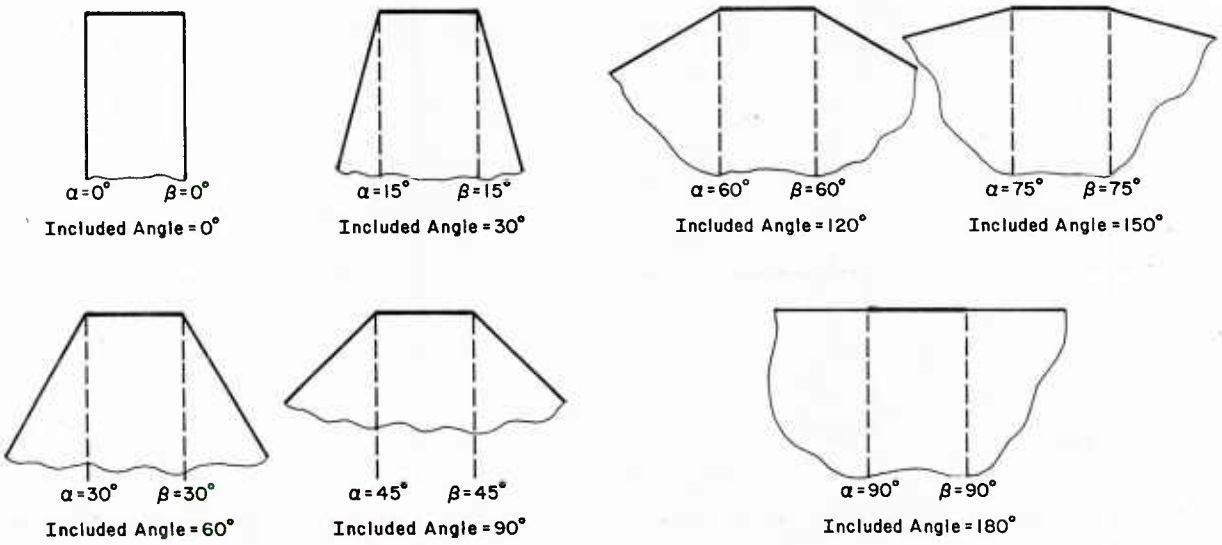

a. Symmetrical shapes with $\alpha+\beta \leq 90°$. b. Symmetrical shapes with $\alpha+\beta>90°$.

Figure 2. Geometrical shapes of the ice sheets that were used in both theoretical and experimental studies.

sumed to be linearly proportional to the deflection of the ice sheet, and the reactive forces at adjacent points in the foundation are assumed to be uncoupled, i.e. a Winkler-type foundation is used. The assumption of a linear foundation is valid as long as the ice sheet does not submerge completely under the water surface or emerge completely out of the water. Thus, this assumption is valid for the linear stability analysis to determine the bifurcation load. As a result of those assumptions a differential equation can be derived that describes the buckling behavior of a floating ice sheet. This partial differential equation is solved by the finite element method. The solution of that equation yields the buckling load and mode of buckling of the floating ice sheet.

The experimental program consisted of pushing ice sheets of different configurations against a structure and measuring the buckling load. The geometrical shapes considered in this study for both the experimental and the theoretical work are shown in Figure 2. These shapes were chosen to cover a wide range of angles; the results for the intermediate shapes may be determined by interpolation.

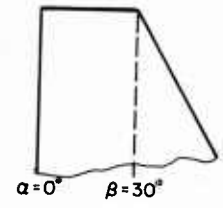

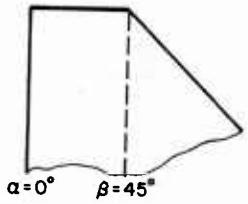

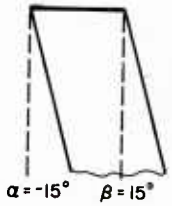

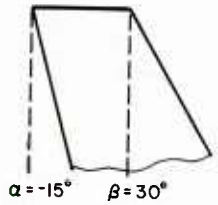

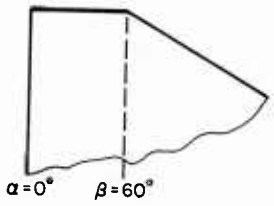

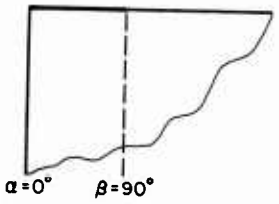

c. Unsymmetrical shapes with α=0°.

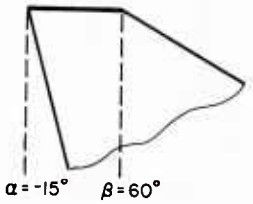

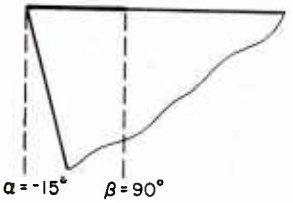

d. Unsymmetrical shapes with α=-15°.

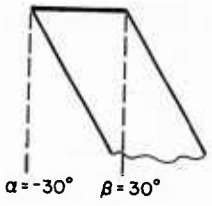

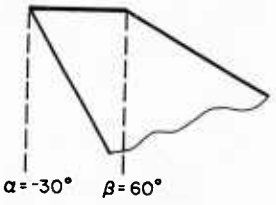

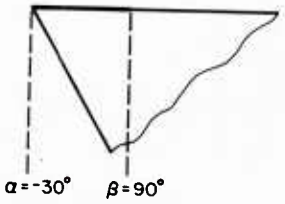

e. Unsymmetrical shapes with α=-30°.

Figure 2 (cont'd).

Literature review

The buckling analysis of infinite beams on elastic foundations was presented by Hetenyi (1946). Aside from this early work the buckling analysis of floating ice sheets was virtually ignored until the past few years.

Sodhi and Hamza (1977) presented a stability analysis of a semi-infinite floating ice sheet, which was performed by the finite element method. Kerr (1978) presented a buckling analysis of a tapered beam of ice. Takagi (1978)

solved the buckling problem of an infinite floating ice sheet uniformly stressed along the periphery of an internal hole. Wang (1978) presented a buckling anaylsis of a semi-infinite ice sheet moving against a vertical, rigid, cylindrical structure; the finite difference method was used for that analysis.

Nevel (1979) obtained a closed form solution to the differential equation that governs the buckling behavior of a tapered beam of ice floating on water. This analysis, as well as the analysis presented by Kerr (1978), was based on beam theory. Sodhi (1979) presented a buckling analysis of a semi-infinite wedge-shaped ice sheet, based on plate theory.
The analysis was performed by the finite element method. In that report Sodhi quantified the relationship between the buckling load of a wedge-shaped ice sheet and the parameters that it is dependent on, i.e. boundary conditions, aspect ratio and included angle.

In 1980 a review of buckling analyses was presented by Sodhi and Nevel. This report compared the results of several of the reports previously mentioned.

All of these reports were based on elastic linear stability theory. Therefore, the buckling loads computed by these analyses are the loads at which bifurcation of equilibrium occurs, not the failure loads of the ice sheets. Kerr (1981a) presented a buckling analysis based on large deformation theory (i.e. the assumption of small deformations used in linear stability analyses was not made).

Sodhi et al. (1982a) conducted an experimental study of the buckling loads required for ice sheets to fail. The ice sheets were pushed against structures of different widths, and the force required for the ice sheets to fail in the buckling mode was measured. Sodhi (1983) also presented a dynamic buckling analysis of a floating ice sheet.

There has also been some work done in fields other than ice engineering that addresses the problem of a thin plate on an elastic foundation. Vlasov and Leont'en (1966) discussed buckling analyses of beams, plates and shells resting on elastic foundations. The solutions presented in that paper considered only the simply supported boundary conditions. The results of a few numerical analyses are presented in the Handbook of Structure Stability (Column Research Committee of Japan 1971).

STATEMENT OF THE PROBLEM

The governing differential equation for the buckling behavior of a thin plate on an elastic foundation can be written as follows (Timoshenko and Gere 1961):

$$D\nabla^4 w + Kw = N_{xx}\frac{\partial^2 w}{\partial x^2} + 2N_{xy}\frac{\partial^2 w}{\partial x\,\partial y} + N_{yy}\frac{\partial^2 w}{\partial y^2} \tag{1}$$

where w = out-of-plane deflection of the plate (ice sheet)

x, y = Cartesian coordinates on the mid-plane of the plate (ice sheet)

∇^4 = biharmonic operator

N_{xx}, N_{xy}, N_{yy} = in-plane stress resultants (force per unit length) which are linearly dependent on the total in-plane external force P.

K = modulus of the foundation (specific weight of water in the case of a floating ice sheet)

$D = E\,h^3/12(1-\nu^2)$, flexural rigidity of the plate (ice sheet)

E = "effective" elastic modulus of the ice sheet

h = ice thickness

ν = Poisson's ratio for ice.

Equation 1 is solved by first solving a plane stress problem to determine the in-plane stress resultants N_{xx}, N_{xy} and N_{yy}, and then solving the eigenvalue problem to determine the buckling loads and modes of buckling. The nondimensional form of the buckling load is found by normalizing the coordinates x and y with respect to the characteristic length of the plate L

$$L = \left[\frac{Eh^3}{12(1-\nu^2)K}\right]^{1/4} \tag{2}$$

to obtain $\underline{x} = x/L$ and $\underline{y} = y/L$. The governing equation can now be rewritten in the following form:

$$\nabla^4 w + w = \frac{P}{BKL^2}\left(N_{\underline{xx}}\frac{\partial^2 w}{\partial \underline{x}^2} + 2N_{\underline{xy}}\frac{\partial^2 w}{\partial \underline{x}\,\partial \underline{y}} + N_{\underline{yy}}\frac{\partial^2 w}{\partial \underline{y}^2}\right) \tag{3}$$

where P = total in-plane buckling load

B = width over which P is distributed at the boundary of the domain

$N_{\underline{xx}}, N_{\underline{xy}}, N_{\underline{yy}}$ = nondimensional expressions ($N_{xx}B/P$, $N_{xy}B/P$, $N_{yy}B/P$).

Solutions of eq 3 that satisfy homogeneous boundary conditions yield the eigenvalue P/BKL^2 (nondimensional buckling load) and the corresponding eigenmode (i.e. mode of buckling).

FINITE ELEMENT ANALYSIS

The stability analysis of a plate on an elastic foundation breaks down into two separate analyses, an in-plane analysis and an out-of-plane analysis. The in-plane analysis determines the stress distribution within the plate, which is described by the in-plane stress resultants obtained in the analysis. The formulation of the out-of-plane problem culminates in an eigenvalue problem. The solution of this problem for the lowest eigenvalue will yield the lowest buckling load and a vector of displacement repre senting the buckling mode.

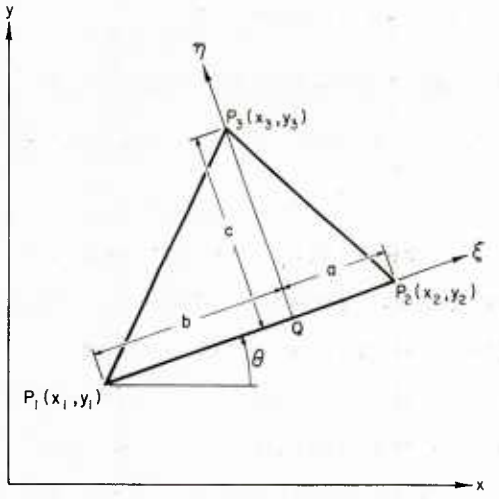

Figure 3. The in-plane and out-of-plane finite element and its coordinate system.

In-plane analysis

The element used in the in-plane analysis is an arbitrary triangular element. The triangular shape was chosen for its effectiveness in modeling the wedge-shaped ice sheets that will be analyzed. The element and its coordinate system are shown in Figure 3. The x,y and ξ,η coordinate systems represent the global and local coordinate systems, respectively. The dimensions a, b and c shown in Figure 3 are given by

$$\begin{aligned} a &= [(x_2-x_3)(x_2-x_1) + (y_2-y_3)(y_2-y_1)]/r \\ b &= [(x_3-x_1)(x_2-x_1) + (y_3-y_1)(y_2-y_1)]/r \\ c &= [(x_2-x_1)(y_3-y_1) - (x_3-x_1)(y_2-y_1)]/r \end{aligned} \tag{4}$$

where

$$r = [(x_2-x_1)^2 + (y_2-y_1)^2]^{1/2} .$$

The x,y coordinates of the vertices are numbered as shown in Figure 3.

The strain energy expression U_e used in developing the plane stress element may be written as follows (Cowper et al. 1970):

$$U_e = \frac{Eh}{2(1-\nu^2)} \iint \left[\left(\frac{\partial u}{\partial \xi}\right)^2 + \left(\frac{\partial v}{\partial \eta}\right)^2 + 2\nu \frac{\partial u}{\partial \xi}\frac{\partial v}{\partial \eta} + \frac{1}{2}(1-\nu)\left(\frac{\partial u}{\partial \eta} + \frac{\partial v}{\partial \xi}\right)^2\right] d\xi d\eta \tag{5}$$

where u is the displacement in the ξ direction, and v is the displacement in the η direction.

The displacement functions used to represent the u and v displacements within an element are

$$u = a_1 + a_2\xi + a_3\eta + a_4\xi^2 + a_5\xi\eta + a_6\eta^2 + a_7\xi^3 + a_8\xi^2\eta + a_9\xi\eta^2 + a_{10}\eta^3$$

$$v = a_{11} + a_{12}\xi + a_{13}\eta + a_{14}\xi^2 + a_{15}\xi\eta + a_{16}\eta^2 + a_{17}\xi^3 + a_{18}\xi^2\eta + a_{19}\xi\eta^2 + a_{20}\eta^3. \quad (6)$$

The finite element derived using these displacement functions is a 20-degree-of-freedom element. There are six degrees of freedom at each of the three vertices of the element. These are u, $\frac{\partial u}{\partial \xi}$, $\frac{\partial u}{\partial \eta}$, v, $\frac{\partial v}{\partial \xi}$ and $\frac{\partial v}{\partial \eta}$. There are also two degrees of freedom (u and v) at the centroid of the element, which are eliminated by a static condensation procedure.

The displacement functions used in developing this element will lead to strain energy convergence rates proportional to n^{-6}, where n is the number of elements per side of a structure.

By utilizing these shape functions and the strain energy expression presented above, the elements of the stiffness matrix can be represented by closed form expressions. For a complete derivation of the element, see Cowper et al. (1970).

Out-of-plane analysis

The element used in the out-of-plane analysis is also an arbitrary triangular element. The coordinate system for the out-of-plane element is identical to that used for the in-plane element (Fig. 3).

The strain energy expression for the stability analysis may be written as follows (Gallagher 1975):

$$U_e = \frac{1}{2} D\iint\left[\left(\frac{\partial^2 w}{\partial \xi^2}\right)^2 + \left(\frac{\partial^2 w}{\partial \eta^2}\right)^2 + 2\nu \frac{\partial^2 w}{\partial \xi^2}\frac{\partial^2 w}{\partial \eta^2} + 2(1-\nu)\left(\frac{\partial^2 w}{\partial \xi \partial \eta}\right)^2\right] d\xi d\eta + \frac{1}{2}\int K w^2 d\xi d\eta$$
$$+ \frac{1}{2}\iint\left[\sigma_{\xi\xi}\, t\left(\frac{\partial w}{\partial \xi}\right)^2 + \sigma_{\eta\eta}\, t\left(\frac{\partial w}{\partial \eta}\right)^2 + 2\sigma_{\xi\eta} t\left(\frac{\partial w}{\partial \xi}\right)\left(\frac{\partial w}{\partial \eta}\right)\right] d\xi d\eta \quad (7)$$

where w is the out-of-plane deflection and σ refers to the stresses resulting from the applied axial load (tensile stress is defined as positive).

The displacement function used to represent the out-of-plane deflection within an element is

$$w(\xi,\eta) = a_1 + a_2\xi + a_3\eta + a_4\xi^2 + a_5\xi\eta + a_6\eta^2 + a_7\xi^3 + a_8\xi^2\eta + a_9\xi\eta^2 + a_{10}\eta^3 + a_{11}\xi^4 + a_{12}\xi^3\eta + a_{13}\xi^2\eta^2 + a_{14}\xi\eta^3 + a_{15}\eta^4 + a_{16}\xi^5 + a_{17}\xi^3\eta^2 + a_{18}\xi^2\eta^3 + a_{19}\xi\eta^4 + a_{20}\eta^5. \quad (8)$$

By substituting eq 8 into eq 7, we may derive the stiffness and geometric matrices for the element.

The finite element derived using the displacement function presented in eq 8 is an 18-degree-of-freedom element. There are six degrees of freedom at each vertex of the triangle. These are the transverse deflection and its first and second derivatives, i.e.

$$w \quad \frac{\partial w}{\partial \xi} \quad \frac{\partial w}{\partial \eta} \quad \frac{\partial^2 w}{\partial \xi^2} \quad \frac{\partial^2 w}{\partial \xi \partial \eta} \quad \frac{\partial^2 w}{\partial \eta^2} .$$

The displacement function used in developing this element is a quintic polynomial in x and y. Therefore, the deflection along any edge of the element varies as a quintic polynomial in the edgewise coordinate.

The general quintic polynomial in two variables depends on 21 constants. Since there are only 18 degrees of freedom, 3 additional constraints may be satisfied: the slope normal to each edge must be a cubic function of the edgewise coordinate. The four coefficients of the cubic polynomial are uniquely determined by the slope normal to the edge and, by the twist, at each of the two terminal vertices. Therefore, the continuity of displacements and normal slopes are maintained across interelement boundaries.

The accuracy of the out-of-plane element is comparable to the accuracy of the in-plane element. This is very desirable because the accuracy of the results of the in-plane analysis will affect the accuracy of the out-of-plane analysis. For a complete derivation of the element, see Cowper et al. (1969).

The finite element formulation of the linear stability analysis of a plate on an elastic foundation may be derived by utilizing the theory of stationary potential energy. By employing the principle of stationary potential energy and following a well-established procedure (Gallagher 1975), the following equation may be derived:

$$[K]\{\Delta_f\} = \lambda[KG]\{\Delta_f\} \tag{9}$$

where

$[K]$ = stiffness matrix

$[KG]$ = geometric stiffness matrix

$\{\Delta_f\}$ = vector of displacements (the eigenvector)

λ = multiplication factor (the eigenvalue) .

Equation 9, which is formulated in the out-of-plane analysis, is in the form of an eigenvalue problem. The solution of eq 9 yields the buckling load λ and the buckling mode $\{\Delta_f\}$.

Two finite element computer programs have been written for this project. The first program (POEF1) was written to solve the in-plane stress problem. POEF1 utilizes the in-plane stress element previously discussed. The second program (POEF2) was written to formulate the out-of-plane problem. POEF2 utilizes the out-of-plane element previously discussed. A third program was an in-plane stress program that utilized a triangular element with a linear displacement function. This program was taken from Desai and Abel (1972).

The finite elements used in POEF1 and POEF2 were chosen for their proven high accuracy and good error-convergence rates. Since the out-of-plane analysis is affected by any errors in the in-plane analysis, it is also desirable that the elements used both have the same strain-energy convergence rates.

The finite element programs used for this project were thoroughly tested. Each of the three programs was used to analyze problems for which an analytical solution was available. The results were very good. The solutions given by the computer programs agreed with the analytical solutions, and the convergence properties appeared to be very good.

Reduction of the eigenvalue problem

The out-of-plane analysis culminates in an eigenvalue problem in the form of eq 9, which is solved by two methods. The first method involves solving the full-sized eigenvalue problem. This requires a very effective solution algorithm and also places restrictions on the size of the problems. Therefore, only selected problems are solved by the first method.

The second method includes an algorithm to reduce the size of the eigenvalue problem. In this method, known as the Guyan reduction method (Guyan 1965), some degrees of freedom are designated as masters and some as slaves. The degrees of freedom retained in the reduced eigenvalue problem are defined as the masters. The Guyan reduction method utilizes the static relationship between the masters and the slaves to remove the slave degrees of freedom while preserving the total strain energy of the structure. The problem of selecting the masters is overcome by employing a recently developed algorithm that allows an analytical selection of the masters. The second method significantly reduces the size of the eigenvalue problem while preserving the accuracy of the eigenvalues of interest.

The following is a presentation of the algorithm used for the analytical selection of the masters. This algorithm, along with a more thorough explanation of its use, can be found in Shah and Raymund (1982). The eigenvalue problem to be solved is in the form of eq 9.

Step 1. Select a cut-off value of λ, to be known as λ_c.

Step 2. Find the degree of freedom for which the ratio of $K_{ii}/KG_{ii} = \lambda$ is the largest. If several degrees of freedom have the same value of the ratio, choose the one with the lowest index.

Step 3. If this value is greater than λ_c, condense this degree of freedom from the stiffness and geometric stiffness matrices by the Guyan reduction procedure.

Step 4. Apply steps 2 and 3 to the reduced matrices obtained.

Step 5. If the greatest value of the ratio K_{ii}/KG_{ii} is $\leq \lambda_c$, stop the procedure at this point and use the reduced matrices obtained to calculate the eigenvalues and eigenvectors of interest.

This algorithm has been used in dynamic natural frequency analyses and has met with a great deal of success (Shah and Raymund 1982). POEF2 utilizes this algorithm to reduce the size of the eigenvalue problem.

Development of the finite element model

The selection of the finite element model is a crucial step in an analysis because the results can be greatly affected by the characteristics of the model. The finite element models used for this project were developed by using several different models to analyze the same problem. The error introduced by varying the level of discretization was determined by comparing the results from the different models. The models used in the analysis were chosen for their ability to accurately describe the behavior of the ice sheet in spite of the following considerations.

1) A finite-sized model is used to represent the behavior of a semi-infinite ice sheet. Therefore, the model must be large enough so that the solution is not significantly affected by changes in boundary conditions at the edges, which are supposed to be at infinity. However, the model has to be small enough so that the solution will be computationally feasible.

2) The discretization of the structure must be designed so that areas with large stress and displacement gradients are highly discretized.

3) The in-plane stress programs calculate the in-plane stress resultants at the centroids of the finite elements. Therefore, if the element is too

large, the values of the in-plane stress resultants will not be representative of the stresses in the area covered by the element.

It is obvious that the solution is affected by the size and number of elements in the model. It is advantageous, then, to analyze the symmetrically shaped ice sheets and the unsymmetrically shaped ice sheets separately.

Finite element model for the symmetrical shapes

Symmetrically shaped ice sheets, i.e. wedges, have been analyzed previously by other researchers. However, the previous analyses used closed form expressions to describe the distribution of in-plane stresses. In the analysis presented here, a separate in-plane finite element analysis is performed to ascertain the distribution of in-plane stresses within the element. Because of the generality of the finite element method, loading distributions can be chosen that more closely simulate conditions that might occur in nature or, as in this case, conditions existing during model studies.

The finite element model used to analyze one of the symmetrical shapes is shown in Figure 4. Figure 5 shows the boundary conditions and the load distribution used in the in-plane analysis. The edge that is supposed to go to infinity is fixed in the x direction but is free to displace in the y direction. Since the wedge is symmetrical about its longitudinal axis, only half of the wedge is modeled. Along the centerline the model is fixed in the

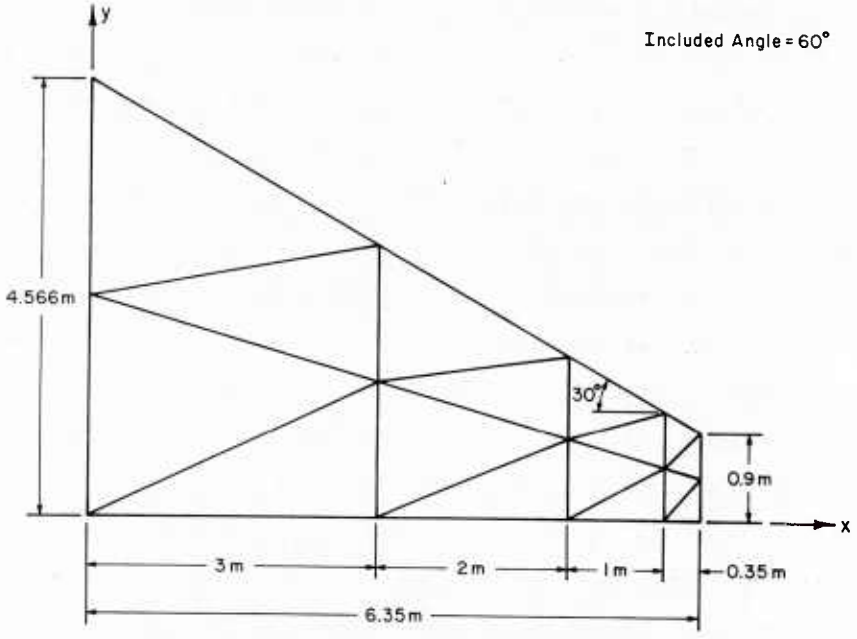

Figure 4. Finite element model used to analyze symmetrically shaped ice sheets.

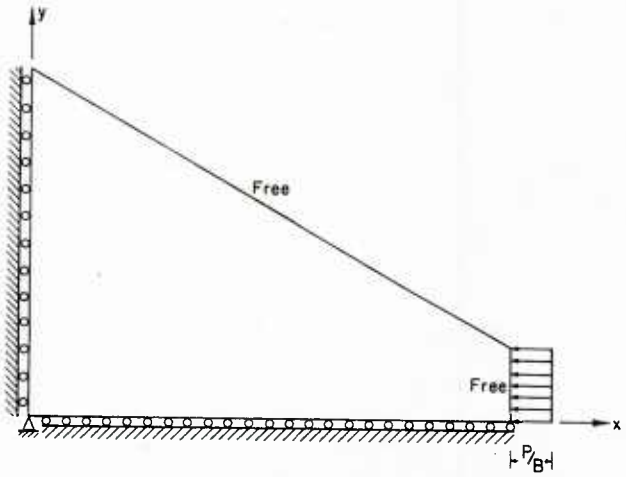

Figure 5. Boundary conditions and load distribution used in the in-plane analysis of the symmetrical shapes. The rollers represent zero normal displacement and zero tangential force at the boundary. The uniformly distributed in-plane load intensity P/B is applied at the ice/structure interface.

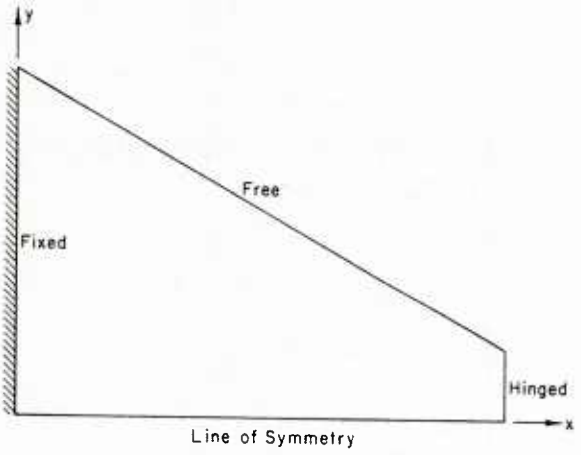

Figure 6. Boundary conditions used in the out-of-plane analysis of the symmetrical shapes. The free boundary condition signifies zero bending moment and zero effective shear force at the boundary. The fixed boundary condition signifies zero deflection and zero normal slope.

y direction due to symmetry but is free to deform along the x axis. The boundary conditions on the loaded edge and the tapered edge are modeled as free.

The loading distribution used in the analysis is uniform. Since the results of the theoretical analysis will be compared to the experimental results from the model study, the loading was chosen to represent the loading that the ice sheets experienced during the tests. The true loading distribution the ice sheets experienced is actually unknown, but the authors feel that the uniformly distributed load is a good assumption.

There are three boundary conditions used in the out-of-plane analysis (Fig. 6):

Free: moment (M) = 0, shear(V) = 0

Fixed: displacement (w) = 0, slope ($\partial w/\partial x$) = 0

Hinged: displacement (w) = 0, moment (M) = 0 .

The edge that is supposed to go to infinity is modeled as fixed. Since the ice sheet is symmetrical about its longitudinal axis, only half of the ice sheet is analyzed. The boundary condition along the centerline is free. However, due to symmetry the slope normal to the centerline is set to zero.

The boundary condition along the tapered edge is modeled as free. The boundary along the loaded edge is modeled as a hinged boundary.

Finite element model for the unsymmetrical shapes

A finite element model used to analyze one of the unsymmetrical shapes is shown in Figure 7. The boundary conditions and load distribution used in the in-plane analysis of an unsymmetrical ice sheet are shown in Figure 8. The edge that is supposed to go to infinity is modeled as fixed in the x direction, but it is free to displace in the y direction. The loaded edge is modeled as free to move in both the x and y directions. The in-plane displacements in the direction perpendicular to the cracks were assumed to be zero, as the ice across the crack can prevent the displacement in the normal but not in the tangential direction.

The shape of the unsymmetrical ice sheet and the loading configuration are such that the ice sheet will experience a moment as well as a compressive load (Fig. 9). The in-plane boundary condition at the cracks is to allow displacement in the tangential direction (slip) and no displacement in the normal direction due to the presence of adjoining ice. The magnitude of the moment experienced by the ice sheet depends on the shape of the distributed loading applied. The authors chose to model this loading as a trapezoidal load. There are now two unknowns that pertain to the loading distribution: the magnitude of the uniform portion of the trapezoidal load and the slope of the top side of the trapezoid (Fig. 8). These two variables (b and θ) cannot be solved for without additional information.

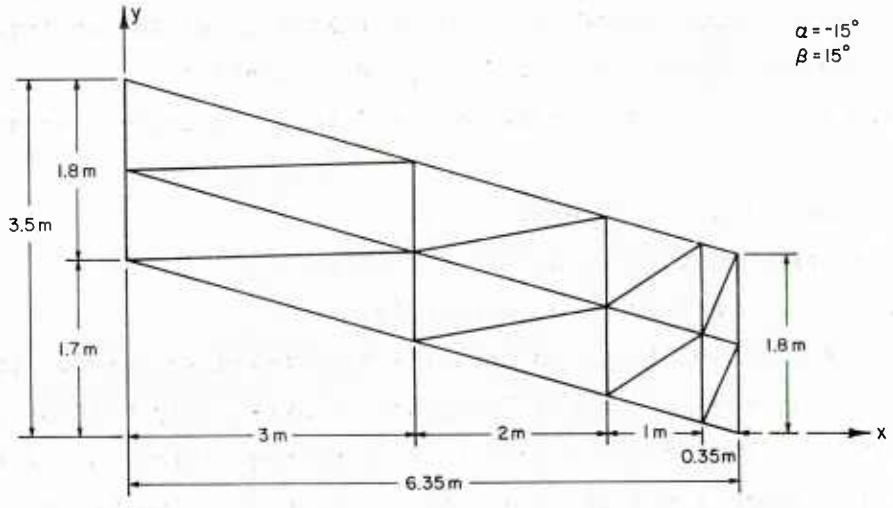

Figure 7. One of the finite element models used to analyze the unsymmetrical shapes.

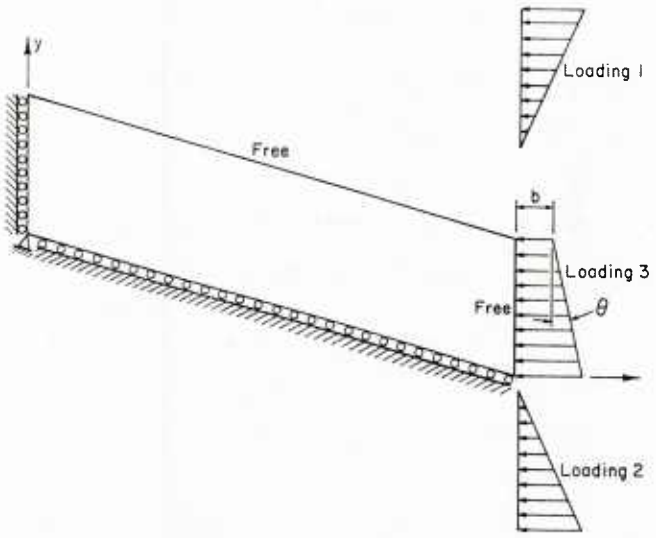

Figure 8. Boundary conditions and in-plane loading distributions used in the in-plane analysis of the unsymmetrical shapes.

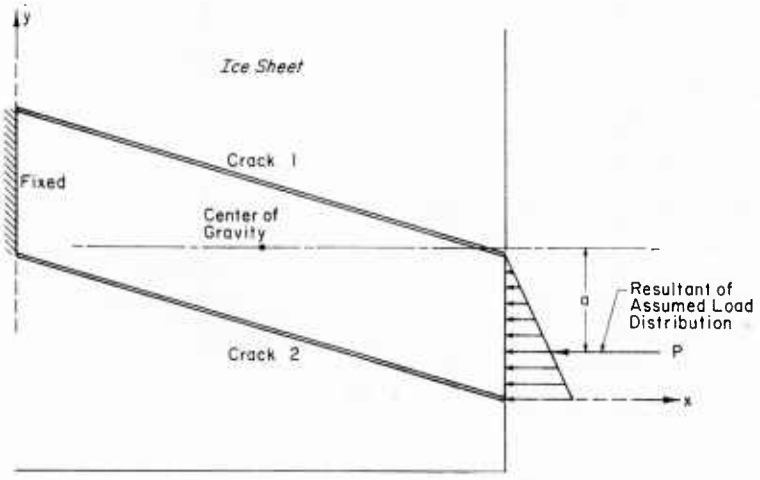

Figure 9. Moment induced by the unsymmetrical shape and the partially confined in-plane boundary conditions used as a consequence of that moment.

Two methods of dealing with this problem were investigated. In one case the additional information needed to solve for b and θ was taken from the experimental force records. In the second method the loading distributions that gave the largest and smallest buckling pressures were used. This method yielded two curves, one representing the largest force that the ice sheet would exert on the structure and the other the minimum force required for the ice sheet to fail. Results were computed for both of these methods. How-

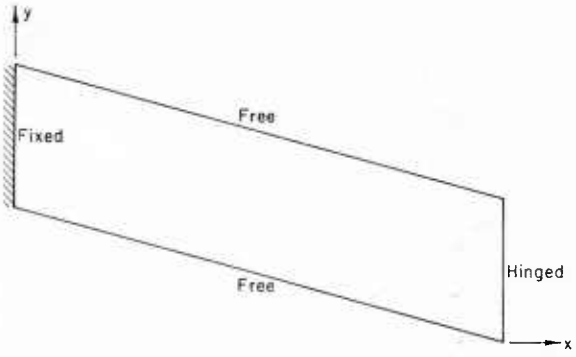

Figure 10. Boundary conditions used for the out-of-plane analysis of the unsymmetrical shapes.

ever, the authors favor the second method since more useful information can be presented without introducing further sources of error.

An example of the boundary conditions used in the out-of-plane analysis for the unsymmetrical shapes is shown in Figure 10. The boundary conditions used for the out-of-plane analysis are the following: hinged at the loaded edge, fixed at the edge that is supposed to go to infinity, and free on the remaining two edges.

EXPERIMENTAL PROCEDURE

The model study presented in this report was performed in the refrigerated test basin at CRREL (Sodhi and Adley 1984). The ice sheets tested were grown by seeding and freezing a solution of 1% urea in water at an ambient temperature of -12°C. Prior to the tests the refrigerated room was warmed up and the temperature of the ice was allowed to stabilize at 0°C. The ice tested can be characterized as columnar ice with horizontal c-axes.

The model study consisted of monitoring the horizontal forces while either pushing a structure against a stationary ice sheet or pushing an ice sheet against a stationary structure. The relative velocity between the structure and the ice sheet was held constant at 1 cm/s. In both cases the length of the structure/ice interface was 1.85 m. The experimental set-up is shown in Figure 11.

Prior to the tests the thickness, flexural strength and characteristic length of the ice sheet were measured. The characteristic length was determined so that the experimental results could be compared to the theoretical results. The procedure involves placing dead weights in discrete increments on the ice sheet and monitoring its deflection. This procedure is described by Sodhi et al. (1982a).

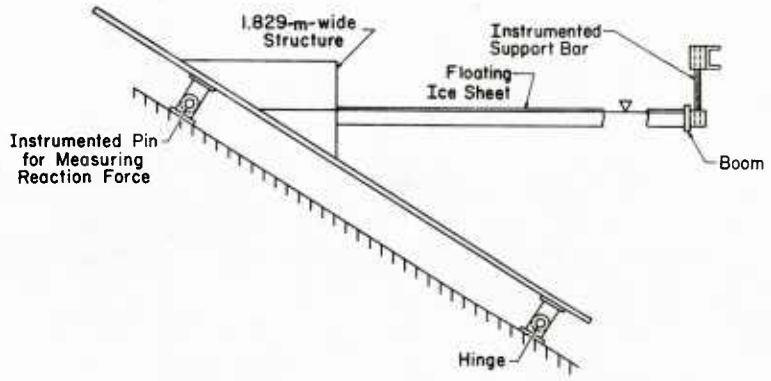

a. Side view.

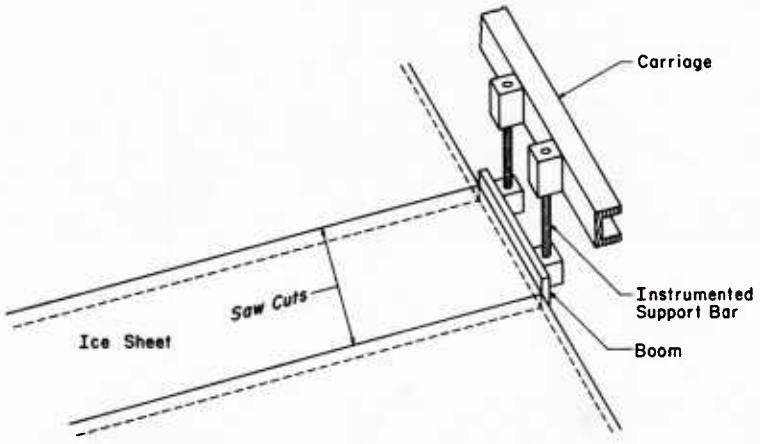

b. Schematic view.

Figure 11. Experimental set-up used in the model study.

The edge of the ice sheet was sawed parallel to the structure prior to testing to ensure uniform, continuous contact. The geometric shape of the ice sheet was modified by cutting two slots with a saw. An example of these slots is shown in Figure 12 (the slots are marked by the black-and-white-striped poles). The far edge of the ice sheet was left intact. A 3-mm-thick rubber pad was attached to the structure where the structure/ice interface would occur during the tests. The pad prevented the edge of the ice sheet from moving up or down but left it free to rotate, creating a hinged boundary condition. This condition was chosen because it could be simulated in the experiments quite accurately.

The only difference between tests was the orientation of the two slots, which were cut to modify the shape of the ice sheet. Thus, the only parameter varied was the geometric shape. The buckling load was assumed to

a. Symmetrical ice sheet prior to testing.

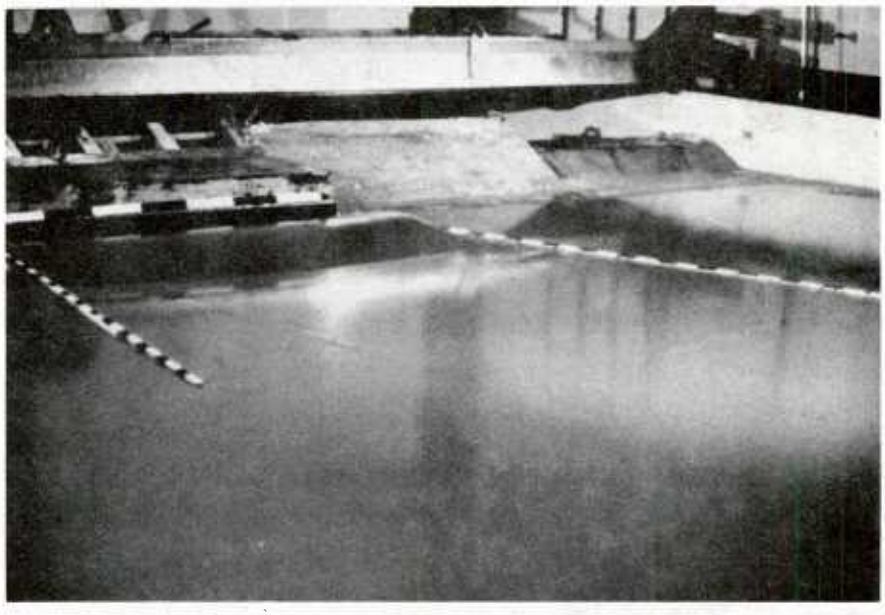

b. Symmetrical ice sheet during testing.

Figure 12. Ice sheet buckling tests.

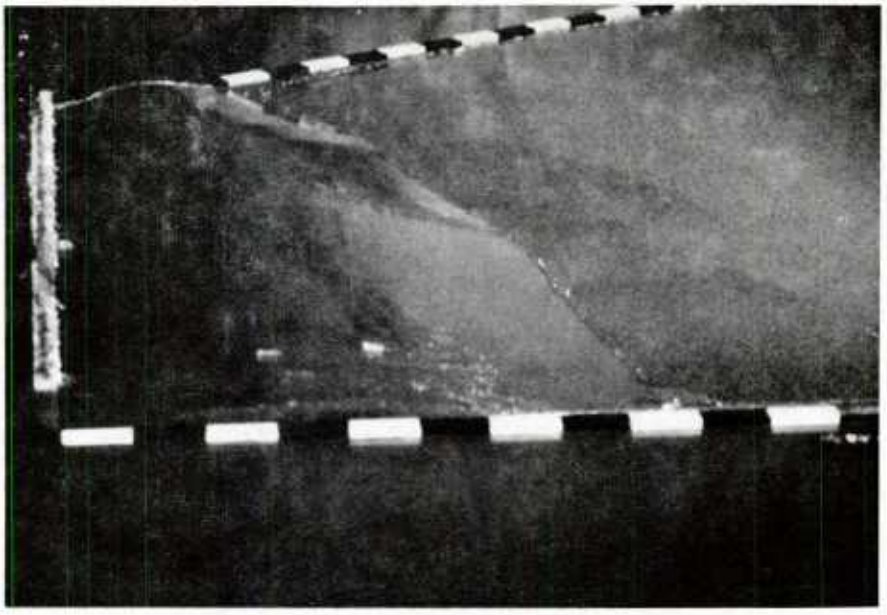

c. Unsymmetrical ice sheet during testing.

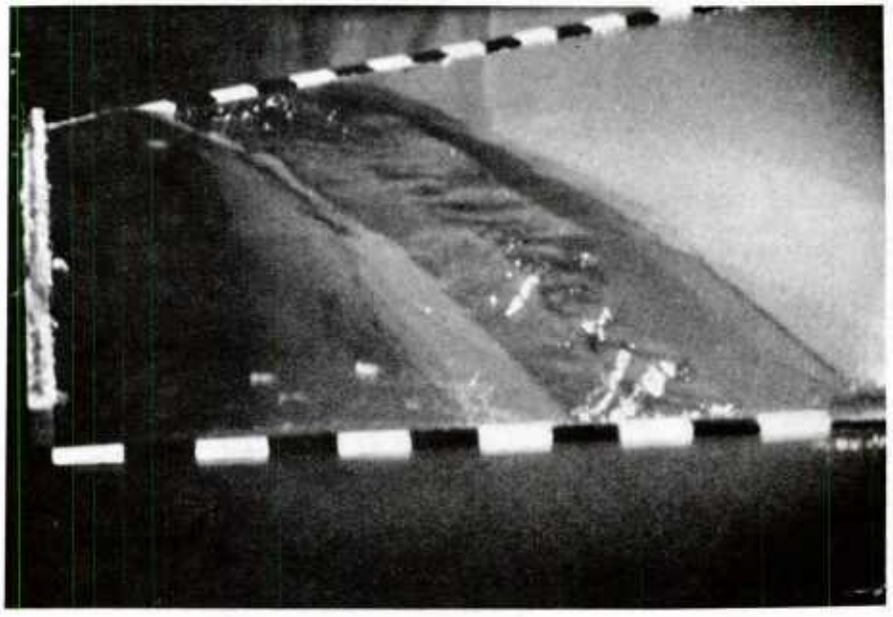

d. Unsymmetrical ice sheet after testing.

Figure 12 (cont'd).

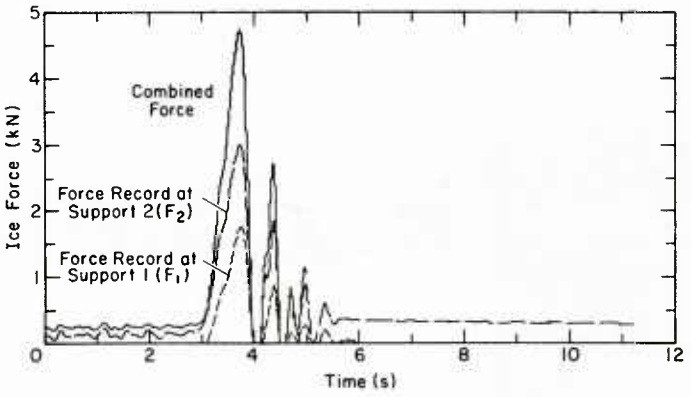

Figure 13. Typical ice forces measured at the two supports in the model study.

be the largest (peak) force exerted on the structure by the ice sheet as determined from the experimental force records (Fig. 13).

RESULTS

The nondimensional buckling load (P/BKL^2) is a function of the boundary conditions, the included angle, and the aspect ratio. For the theoretical analysis the boundary conditions and the aspect ratio were held constant. Thus, the results presented will show the effect that the geometry of the ice sheet has on the nondimensional buckling load. The boundary conditions used in the theoretical analysis were chosen to simulate the boundary conditions used in the model study, so the results of the theoretical analysis can be compared to the experimental results.

Symmetrical shapes

The results of the analyses of the symmetrically shaped ice sheets are presented in Figure 14. The experimental results are also presented in Table 1, along with data on ice sheet and test conditions. In approximately 90% of the tests the aspect ratio of the ice sheet is very close to that used in the theoretical analysis (4.3). Thus, there is a strong basis for comparison between most of the points and the curves developed in the theoretical analysis.

The three curves presented in Figure 14 represent separate theoretical analyses but use the same aspect ratio and boundary conditions. Two of the curves, representing the results of two finite element stability analyses, were computed for this project. For the first analysis (represented by curve 1) a triangular-shaped element utilizing a cubic displacement function was

Table 1. Results of the experiment on symmetrically shaped ice sheets.

Test no.	Included Angle (degrees)	h (cm)	L (m)	B (m)	P (N)	B/L	$\frac{P}{BKL^2}$
14	180	3.4	0.46	1.85	10,353.0	4.02	2.697
15	0	3.4	0.46	1.85	9,468.0	4.02	2.466
16	60	3.4	0.46	1.85	8,891.0	4.02	2.316
17	90	3.4	0.39	1.85	8,476.0	4.74	3.072
18	120	3.4	0.39	1.85	9,267.0	4.74	3.358
19	30	3.4	0.39	1.85	6,086.0	4.74	2.206
20	0	3.4	0.35	1.85	4,610.0	5.29	2.074
21	180	3.4	0.35	1.85	8,806.0	5.29	3.962
25	0	2.8	0.475	1.85	11,349.0	3.89	2.773
26	180	2.8	0.475	1.85	12,430.0	3.89	3.037
27	60	2.8	0.45	1.85	7,707.0	4.11	2.098
28	90	2.8	0.435	1.85	9,000.0	4.25	2.622
29	120	2.8	0.43	1.85	9,998.0	4.30	2.981
30	150	2.8	0.43	1.85	8,443.0	4.30	2.517
31	30	2.8	0.43	1.85	9,522.0	4.30	2.839
32	0	2.8	0.43	1.85	5,405.0	4.30	1.629

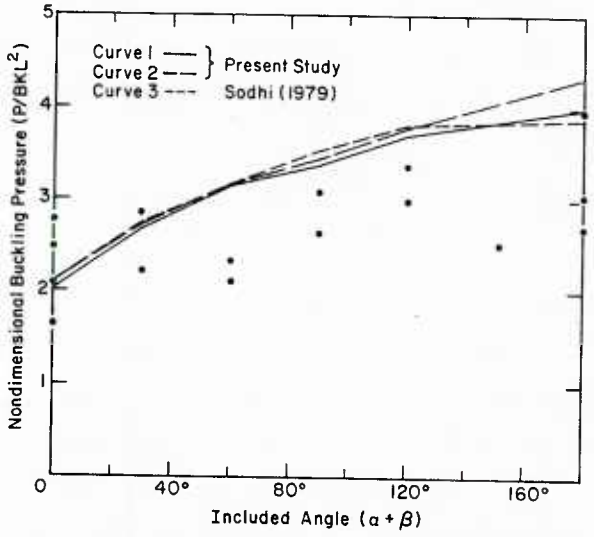

Figure 14. Results of the theoretical (lines) and experimental (points) work on symmetrical shapes. The assumptions for these analyses are described in the text.

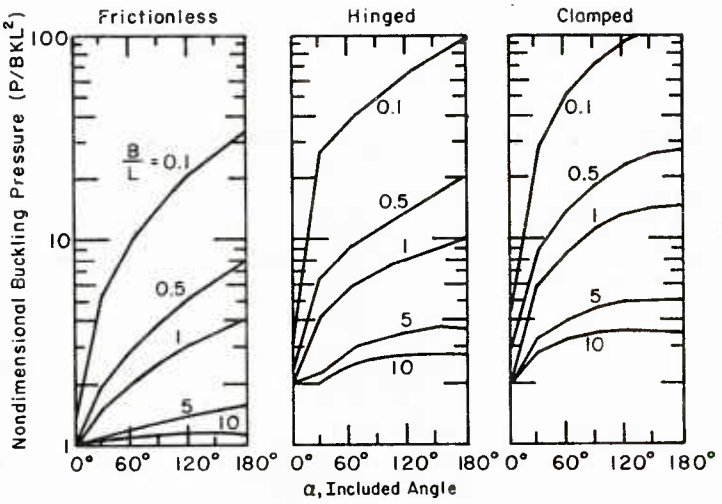

Figure 15. Plot of nondimensional buckling pressure (P/BKL^2) vs included angle $\alpha+\beta$ for different boundary conditions at the ice/structure interface and for different aspect ratios (B/L).

employed for the in-plane stress analysis. This analysis used the computer programs written for this project (POEF1 and POEF2). In the second analysis (represented by curve 2) a triangular-shaped element utilizing a linear displacement function was used for the in-plane stress analysis. This analysis used a plane stress finite element program taken from Desai and Abel (1972) and the out-of-plane program written for this project (POEF2). Both of these analyses used a computer program presented by Gladwell and Tahbildar (1972) that solves the algebraic eigenvalue problem.

The third curve (represented by curve 3) was computed by Sodhi (1979). Sodhi used a Fourier decomposition and the finite element method to solve the buckling problem of the symmetrical shapes. Sodhi's analysis assumes a radial stress field for the in-plane stress distribution.

For a symmetrical configuration of cracks the results of the buckling analysis of the wedge-shaped ice sheet (Sodhi 1979) have been plotted in Figure 15, which shows the normalized buckling loads (P/BKL^2) with respect to the wedge angle ($\alpha+\beta$) for different aspect ratios and boundary conditions at the ice/structure interface.

Unsymmetrical shapes

The results of the analyses of the unsymmetrically shaped ice sheets are presented in Figure 16. The test results are presented in Table 2.

Table 2. Results of the experiment on unsymmetrically shaped ice sheets.

Test no.	Included angles (degrees) α	β	h (cm)	L (m)	B (m)	P (N)	$\frac{B}{L}$	$\frac{P}{BKL^2}$
33	0	0	3.03	0.35	1.85	4,279.0	5.29	1.925
34	0	90	3.03	0.35	1.85	5,034.0	5.29	2.265
35	0	30	3.03	0.35	1.85	4,168.0	5.29	1.875
36	0	60	3.03	0.35	1.85	4,579.0	5.29	2.060
37	0	45	3.03	0.30	1.85	4,742.0	6.17	2.904
38	-30	60	3.03	0.30	1.85	4,775.0	6.17	2.925
55	-15	15	3.10	0.39	1.85	8,592.0	4.74	3.114
56	-15	30	3.10	0.39	1.85	7,911.0	4.74	2.867
57	-15	60	3.10	0.39	1.85	6,305.0	4.74	2.285
58	-15	90	3.10	0.37	1.85	6,262.0	5.00	2.521
59	-30	30	3.10	0.35	1.85	3,614.0	5.29	1.626
60	-30	60	3.10	0.35	1.85	3,658.0	5.29	1.646
61	-30	90	3.10	0.35	1.85	3,405.0	5.29	1.532
69	0	0	2.87	0.32	1.85	5,097.0	5.78	2.744
71	0	60	2.87	0.32	1.85	6,671.0	5.78	3.591
72	0	90	2.87	0.32	1.85	4,245.0	5.78	2.285

The curves presented in Figures 16a and b are the results of the theoretical analyses. The same aspect ratio and boundary conditions were used for each analysis, and the aspect ratio was the same as that used for the symmetrical analyses.

The curves were computed using an in-plane finite element program presented by Desai and Abel (1972) and the out-of-plane program written for this project (POEF2). The program presented by Desai and Abel (1972) utilizes a triangular-shaped element derived by using a linear displacement function. The eigenvalue problem was solved by using the computer program presented by Gladwell and Tahbildar (1972).

The three curves presented in Figure 16 were computed using different loading distributions. Curves 1 and 2 represent, respectively, the largest load the ice sheet can withstand prior to buckling and the minimum load required to buckle the ice sheet. Curve 3 is computed by applying the loading distributions obtained from experimental force records.

There are no results available for the unsymmetrical shapes when $\alpha = -30°$ due to numerical difficulties in obtaining a solution. The cause for these difficulties is not known.

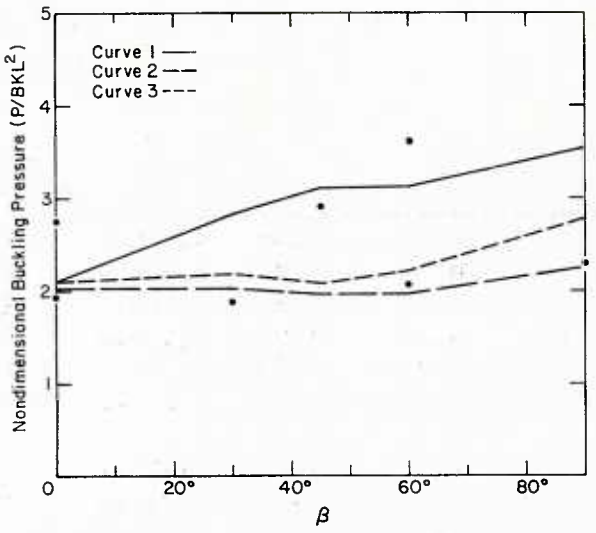

a. $\alpha = 0°$.

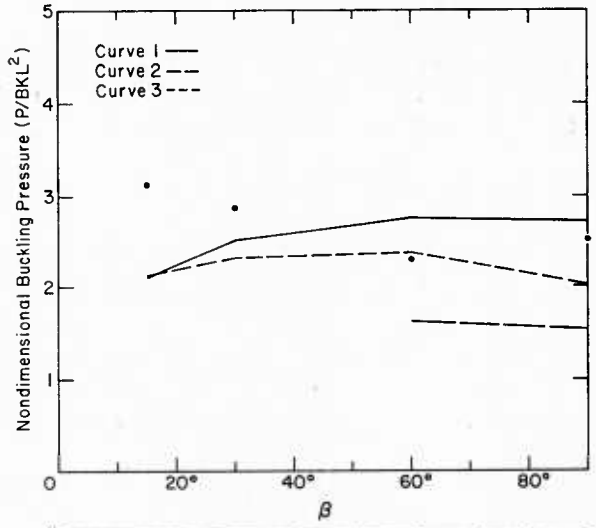

b. $\alpha = -15°$.

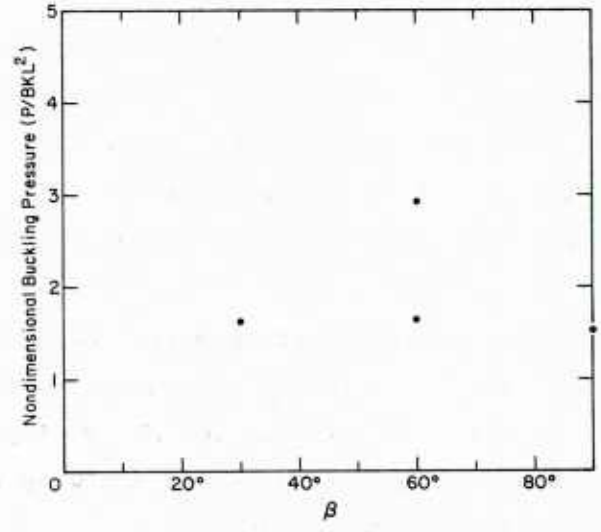

c. $\alpha = -30°$.

Figure 16. Results of the theoretical (lines) and experimental (points) work on unsymmetrical shapes. The theoretical results were obtained by finite element analysis using different assumptions for the distribution of in-plane load.

Mode shapes

Since the load was applied slowly to the ice sheets tested in the model study (1 cm/s), all of the ice sheets buckled in the first mode. The shape of the first mode of buckling predicted by the theoretical analysis appears to agree well with the mode shapes observed in the experimental work.

DISCUSSION AND CONCLUSIONS

The theoretical analyses presented in this report were done for one value of the aspect ratio (structure width/characteristic length). However, the close agreement between the results computed for this project and the results computed by Sodhi (1979) and between the theoretical and experimental results of this project indicate that the analysis developed could be used successfully for ice sheets with different aspect ratios. The comparison between the results presented in this paper and Sodhi's (1979) results also indicates that the assumption of the radial stress field for the distribution of the in-plane stresses is valid for the symmetrical shapes.

The authors believe, after comparing the results of the analyses of the symmetrical shapes, that the use of the higher-order plane stress finite element was not warranted. The results of the stability analyses were not adversely affected by using the less-accurate plane stress computer program taken from Desai and Abel (1972), so it was used for the analyses of the unsymmetrical shapes because it is less expensive to run.

The results of the theoretical and experimental analyses show that the nondimensional buckling load for a symmetrical configuration increases as the included angle increases. Thus, the configuration with the largest buckling load is the symmetrical shape with an included angle of 180°.

The in-plane analysis of the unsymmetrical shapes became quite complex because of 1) the moment induced by the unsymmetrical geometry, 2) the ability of the cracks to transmit compressive normal forces created by that moment, and 3) the fact that the loading distribution, and therefore the magnitude of the applied normal force and moment, is an unknown. Because of that moment, the in-plane analysis was done by modeling the unsymmetrical shapes as partially confined; i.e. no displacements were allowed perpendicular to one longitudinal edge.

Since the actual loading distribution experienced by the ice sheet is an unknown, the analysis used two assumed loading distributions and one loading

distribution determined from the experimental force records. The two assumed loading distributions were chosen to give the maximum and minimum buckling loads. The loading distribution determined from the force record approximates the actual loading distribution. However, since the force records were used to determine that load distribution, it is subject to experimental error.

The discrepancy between the theoretical and experimental results, as well as the scatter in the experimental results, may be due to the following considerations:

1) The nondimensional buckling pressure is a function of the aspect ratio (structure width/characteristic length). Thus, the scatter in the experimental data can be partially attributed to the fact that the aspect ratios were not the same for each test. The discrepancy between the theoretical and experimental results can be partially explained by the fact that the aspect ratio used in the theoretical analysis was rarely equal to the aspect ratios measured during the experimental tests. Since a 10% error in the characteristic length (the structure width was a constant) results in a 20% error in the nondimensional buckling pressure, the differing values used for the characteristic lengths can be a significant source of error.

2) In the theoretical analysis the ice sheet is assumed to be a perfect structure; i.e. there are no imperfections such as initial curvatures, eccentricity of loads, etc., in the ice sheet. Thus, the buckling loads computed in the theoretical analysis are the loads at which bifurcation of equilibrium exists for "perfect" ice sheets. Any imperfection in the sheet or eccentricity in the loading can lead to lower buckling loads in the experiments.

The authors believe that the scatter in the experimental data can largely be attributed to the variations in the ratio of structure width to characteristic length, as the buckling load (P/BKL^2) is most sensitive to this parameter (Fig. 15).

LITERATURE CITED

Column Research Committee of Japan (1971) Handbook of Structure Stability. Tokyo, Japan: Corona Publishing Co.

Cowper, G.R., E. Kosko, G.M. Lindberg and M.D. Olson (1969) Static and dynamic applications of a high-precision triangular plate bending element. American Institute of Aeronautics and Astronautics Journal, 7(10): 1947-1965.

Cowper, G.R., G.M. Lindberg and M.D. Olson (1970) A shallow shell finite element of triangular shape. International Journal of Solids and Structures, 6: 1133-1156.

Desai, C.S. and J.F. Abel (1972) Introduction to the Finite Element Method. New York: Van Nostrand Reinhold Company.

Gallagher, R.H. (1975) Finite Element Analysis Fundamentals. Englewood Cliffs, New Jersey: Prentice Hall.

Gladwell, G.M.L. and U.C. Tahbildar (1972) The algebraic eigenvalue problem - A set of Fortran subroutines. Solid Mechanics Division, University of Waterloo, Waterloo, Ontario, Canada, Report No. 18.

Guyan, R.J. (1965) Reduction of stiffness and mass matrices. American Institute of Aeronautics and Astronautics Journal, 3: 380.

Hetenyi, M.I. (1946) Beams on Elastic Foundations. Ann Arbor, Michigan: University of Michigan Press.

Kerr, A.D. (1978) On the determination of horizontal forces a floating ice plate exerts on a structure. Journal of Glaciology, 20(82): 123-134.

Kerr, A.D. (1981a) On the buckling force of floating ice plates. USA Cold Regions Research and Engineering Laboratory, CRREL Report 81-9.

Kerr, A.D. (1981b) Remarks on the buckling analyses of floating ice sheets. International Association for Hydraulic Research Symposium on Ice, Quebec, Vol. 2, pp. 932-937.

Nevel, D.E. (1979) Bending and buckling of a wedge on an elastic foundation. International Union of Theoretical and Applied Mechanics Symposium on the Physics and Mechanics of Ice, Technical University of Denmark, Copenhagen.

Shah, V.N. and M. Raymund (1982) Analytical selection of masters for the reduced eigenvalue problem. International Journal for Numerical Methods in Engineering, 18(1): 89-98.

Sodhi, D.S. (1979) Buckling analysis of wedge-shaped floating ice sheets. Fifth International Conference on Port and Ocean Engineering Under Arctic Conditions (POAC 79), Trondheim, pp. 797-810.

Sodhi, D.S. and H.E. Hamza (1977) Buckling analysis of a semi-infinite ice sheet. Proceedings, Fourth International Conference on Post and Ocean Engineering Under Arctic Conditions, Memorial University of Newfoundland, St. John's, Newfoundland, Canada, Vol. 1, pp. 593-604.

Sodhi, D.S. and D.E. Nevel (1980) Review of buckling analyses of ice sheets. A state-of-the-art report by the working group on ice forces on structures, IAHR. USA Cold Regions Research and Engineering Laboratory, Special Report 80-26.

Sodhi, D.S., F.D. Haynes, K. Kato and K. Hirayama (1982a) Experimental determination of the buckling loads of floating ice sheets. Presented at the Second Symposium on Applied Glaciology, Hanover, New Hampshire.

Sodhi, D.S., K. Kato, F.D. Haynes and K. Hirayama (1982b) Determining the characteristic length of model ice sheets. Cold Regions Science and Technology, 6(2): 99-104.

Sodhi, D.S. (1983) Dynamic buckling of floating ice sheets. Proceedings, Seventh International Conference on Port and Ocean Engineering Under Arctic Conditions (POAC 83), Helsinki, Finland, April.

Sodhi, D.S. and M.D. Adley (1984) Experimental determination of buckling loads of cracked floating ice sheets. Proceedings, Third International Symposium on Offshore Mechanics and Arctic Engineering, New Orleans, La., February, 1984, Vol. 3, pp. 183-186.

Takagi, S. (1978) The buckling pressure of an elastic plate floating on water and stressed uniformly along the periphery of an internal hole. USA Cold Regions Research and Engineering Laboratory, CRREL Report 78-14.

Timoshenko, S.P. and J.M. Gere (1961) Theory of Elastic Stability. New York: McGraw-Hill.

Vlasov, V.Z. and U.N. Leont'en (1966) Beams, plates and shells on elastic foundations. Israel Program for Scientific Translation, IPST Cat. No. 1453.

Wang, Y.S. (1978) Buckling analysis of a semi-infinite ice sheet moving against cylindrical structures. Proceedings, IAHR Symposium on Ice Problems, Lulea, Sweden.

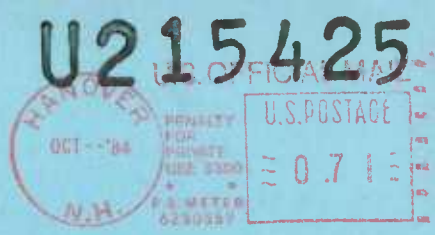

Naval Postgraduate School
ATTN: Dudley Knox Library, Code 0142
Monterey, CA 93943